PHYSICAL REVIEW B **89**, 060202(R) (2014)

Probing the electronic structure of liquid water with many-body perturbation theory

T. Anh Pham,[1,2,*] Cui Zhang,[1,†] Eric Schwegler,[2] and Giulia Galli[3]
[1]*Department of Chemistry, University of California, Davis, California 95616, USA*
[2]*Lawrence Livermore National Laboratory, Livermore, California 94551, USA*
[3]*The Institute for Molecular Engineering, University of Chicago, Chicago, Illinois 60637, USA*
(Received 25 October 2013; revised manuscript received 14 February 2014; published 27 February 2014)

We present a first-principles investigation of the electronic structure of liquid water based on many-body perturbation theory (MBPT), within the G_0W_0 approximation. The liquid quasiparticle band gap and the position of its valence band maximum and conduction band minimum with respect to vacuum were computed and it is shown that the use of MBPT is crucial to obtain results that are in good agreement with experiment. We found that the level of theory chosen to generate molecular dynamics trajectories may substantially affect the electronic structure of the liquid, in particular, the relative position of its band edges and redox potentials. Our results represent an essential step in establishing a predictive framework for computing the relative position of water redox potentials and the band edges of semiconductors and insulators.

DOI: 10.1103/PhysRevB.89.060202 PACS number(s): 79.60.Bm, 31.15.E−, 71.15.Pd, 71.15.Qe

Liquid water occupies a central role in many problems concerning energy use and environmental remediation, including its utilization for solar energy capture and conversion in photocatalytic devices [1]. Yet, surprisingly the electronic properties of water are poorly understood, in spite of their paramount importance in determining the physical and chemical properties of aqueous interfaces, e.g., those with photoelectrodes in water splitting cells. In particular, the determination of basic properties of liquid water, such as the ionization potential and electron affinity remains challenging, from both theoretical and experimental standpoints.

Photoemission spectroscopy (PES) provides information on the valence band structure of liquid water, while inverse photoemission and the use of excess electrons are valuable probes of conduction band energy levels. As discussed, e.g., in Ref. [2], excess electrons may be "presolvated" in liquid water, prior to reaching a solvated state following solvent reorganization. It has been suggested [3,4] that thermal fluctuations of molecular dipole moments may give rise to trap states for presolvated electrons, which are localized below the conduction band minimum (CBM) of neutral liquid water. Thus, understanding the electronic structure of neutral liquid water is also crucial to unravel fundamental processes involving excess electrons, which have been the subject of intense experimental and theoretical studies [2].

One of the first extensive PES studies of the electronic structure of liquid water was conducted by Delahay *et al.* [5,6]. The authors showed that close to the threshold energy E_t, the photocurrent (Y) depends quadratically on the photon energy E, i.e., $Y \sim (E - E_t)^2$, consistent with the theoretical predictions of Brodsky *et al.* [7]. By extrapolating $Y^{0.5}$ to zero, Delahay *et al.* [5,6] found $E_t = 10.06$ eV, i.e., the valence band maximum (VBM) lying 10.06 eV below the vacuum level.

The development of the vacuum liquid microjet technique led to great advances in liquid PES, and in the understanding of the electronic structure of liquids and solutions [8,9]. This approach permits the transfer of electrons to the detector essentially free of collisions with gas-phase water molecules, and thus it provides a more precise measurement of the electronic levels of liquid water. Using microjets, Winter *et al.* [9] reported $E_t = 9.9$ eV for water at ambient conditions. However, we note that this value was derived from a linear extrapolation of the photocurrent in the proximity of the threshold energy; by employing the power law used in Refs. [5,6], one would instead obtain $E_t = 9.3$ eV from the same experimental data. This value is ≈0.7 eV smaller than the one previously reported [5,6], possibly due to a reduction in electron collisions with gas phase water molecules in liquid microjet experiments.

Unlike the VBM position, the CBM of liquid water was inferred only indirectly from solution measurements. Under the assumption that excess electrons are injected into the water conduction band, photoelectron experiments on electrolytes and photoionization experiments of aqueous solutions led to similar values of $V_0 = -1.2$ eV [10,11], i.e., the CBM lying 1.2 eV below the vacuum level. However, we note that excess electrons may initially localize in trap states below the water CBM [3,4], and the value −1.2 eV might not correspond to the position of the CBM of neutral water. An estimate of $V_0 = -0.74$ eV was given based on thermodynamic considerations [4]. By combining the value of $E_t = 9.3$–10.06 eV with $V_0 = -(0.74$–$1.2)$ eV one finds a quasiparticle band gap of $E_t - |V_0| = 8.7 \pm 0.6$ eV [4]. Given the large uncertainty in the experimental measurements, theoretical efforts are needed to provide a fundamental understanding of the electronic structure of liquid water.

In this Rapid Communication, we report results for the band gap and band edge positions of liquid water, obtained by combining *ab initio* and classical molecular dynamics (MD) simulations, and electronic structure calculations within many-body perturbation theory (MBPT). We found that the use of MBPT is essential to obtain results in satisfactory agreement with existing measurements. In addition, we analyzed the effect of structural properties on the electronic structure of water, in particular we compared results for the band edge positions obtained with configurations generated by

*atupham@ucdavis.edu
†Present address: Department of Chemistry, Princeton University, Princeton, New Jersey 08544, USA.

first-principles and classical MD simulations. We note that trap states could be accessed by considering liquid water samples with an explicit excess electron [12]. Since the focus of our work is on the band gap and band edge positions of liquid water, the effect of an excess electron was not considered here.

An accurate determination of the electronic gap and band edge positions of water encompasses several theoretical and computational challenges, in particular: (i) the generation of well-equilibrated MD trajectories to obtain structural models of the liquid; and (ii) the calculation of electronic states of models composed of several hundreds of electrons using advanced electronic structure methods, such as hybrid functionals or many-body perturbation theory, e.g., within the G_0W_0 approximation [13,14]. In particular, calculations at the G_0W_0 level of theory are rather demanding from a computational standpoint, and in the case of water they have been mostly limited to 16-molecule samples [15,16], and only recently 64-molecule cells were used [17]. In addition, MPBT studies were limited to band gaps and absorption spectra, and band edge calculations have not yet been reported for liquid water.

We carried out Born-Oppenheimer *ab initio* MD simulations using the QBOX code [18], with interatomic forces derived from density functional theory (DFT) using the Perdew, Burke, and Ernzerhof (PBE) approximation for the exchange and correlation energy functional [19]. The interaction between valence electrons and ionic cores was represented by norm-conserving pseudopotentials [20], and the electronic wave functions were expanded in a plane-wave basis set truncated at a cutoff energy of 85 Ry. We used a cubic simulation cell containing 64 heavy [21] water molecules at the experimental density and we sampled the Brillouin zone by the Γ point only. The equilibration runs were carried out at constant temperature (NVT conditions) with $T = 390$ K. The neglect of zero-point motion effects [22] of light nuclei and the use of the PBE approximation are known to yield an overstructured liquid water at ambient conditions, and an elevated simulation temperature of $T \approx 400$ K may be used to recover the experimental structure and diffusion coefficients at $T = 300$ K [23,24]. Snapshots employed in G_0W_0 calculations were extracted from a 20 ps trajectory obtained with *ab initio* runs at constant energy (NVE), following the NVT equilibration. Furthermore, to investigate size effects, smaller snapshots with 32 water molecules were also generated with the same simulation protocol.

In addition to configurations obtained from *ab initio* simulations, we considered snapshots of 64 water molecules generated by classical MD with the TIP3P, TIP4P [25], and SPC/E [26] empirical potentials. Classical equilibration runs were carried out at an average temperature of $T = 300$ K, as empirical potentials were designed to reproduce the properties of water at ambient conditions. Snapshots used in G_0W_0 calculations were collected from 10 ns NVE simulations.

The quasiparticle energies (E_n^{qp}) were calculated at the G_0W_0 level of theory [14], as a first-order correction to the Kohn-Sham (KS) energies (ε_n):

$$E_n^{qp} = \varepsilon_n + \langle\psi_n|\Sigma_{G_0W_0}\left(E_n^{qp}\right)|\psi_n\rangle - \langle\psi_n|V_{xc}|\psi_n\rangle, \qquad (1)$$

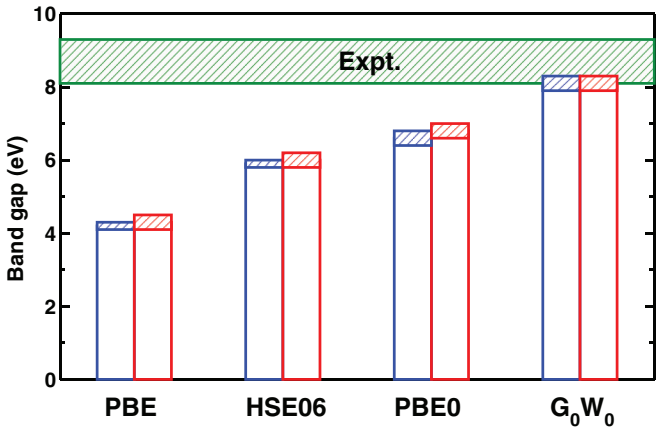

FIG. 1. (Color online) Quasiparticle band gap (eV) of liquid water models generated by *ab initio* MD simulations with 32 (red rectangle) and 64 (blue rectangle) molecule cells, computed at the DFT level of theory with semilocal (PBE) and hybrid functionals (PBE0 [31,32] and HSE06 [33]), and at the G_0W_0 level of theory. The experimental band gap of liquid water is 8.7 ± 0.6 eV. [4] Error bars (standard deviation) of theoretical calculations and experimental results (see text) are indicated by shaded areas.

where V_{xc} is the exchange-correction potential entering the chosen KS Hamiltonian and $\Sigma_{G_0W_0}$ is the self-energy operator, computed from the one particle Green's function (G_0) and the screened Coulomb interaction (W_0). We used the method proposed in Ref. [27] and [28], which does not require the explicit calculation of empty electronic orbitals nor the use of a plasmon-pole model [14]; the convergence of the G_0W_0 calculation is controlled by only one parameter (in addition to the plane-wave cutoff), i.e., the number of eigenpotentials (N_{eig}) used for the spectral decomposition of the dielectric matrix [29,30]. We used $N_{\text{eig}} = 1000$ and we verified that the quasiparticle energies were converged within 0.04 eV. We averaged our results over 10 configurations chosen to be equally spaced in time over a trajectory of 20 ps and of 10 ns for *ab initio* and classical simulations, respectively. In addition to the G_0W_0 approach, hybrid functionals were also employed to compute the band gap for comparison.

Figure 1 presents the results for the quasiparticle band gap of 64- and 32-molecule configurations generated by *ab initio* MD, and computed at different levels of theory. The results appear to be insensitive to the cell size, consistent with previous studies [23,24]. As expected, the PBE functional greatly underestimates the water band gap; although a substantial improvement on the PBE value, the HSE06 and PBE0 band gaps are still lower than the experimental value by $\approx$2.7 eV and $\approx$2.0 eV, respectively. These inaccuracies can be qualitatively understood in term of average dielectric screening. In the case of a condensed system, the appropriate fraction of exact exchange (α) entering the definition of a hybrid functional should be approximately proportional to the inverse of the electronic dielectric constant (ϵ_∞) of the material, i.e., $\alpha \approx 1/\epsilon_\infty$ [34]. For the PBE0 and HSE06 functionals, $1/\alpha = 4$, a value substantially different from $\epsilon_\infty = 1.7$–1.8 [16], hence the gap is underestimated when using these functionals. The best agreement with

experiment was obtained using MBPT, yielding a band gap of 8.1 ± 0.2 eV.

In order to evaluate the band edge positions of the liquid with respect to vacuum ($VBM^{vac.}$ and $CBM^{vac.}$), we adopted a two-step procedure: (i) we computed the band edge positions (VBM^{bulk},CBM^{bulk}), including G_0W_0 corrections (ΔE^{VBM},ΔE^{CBM}), with respect to the average electrostatic potential of a bulk model; (ii) we computed the relative average electrostatic potential (ΔV) of the bulk and vacuum regions, by employing water slabs in contact with a vacuum region. The values $VBM^{vac.}$ and $CBM^{vac.}$ are then given by:

$$\begin{aligned} VBM^{vac.} &= VBM^{bulk} + \Delta E^{VBM} + \Delta V \\ CBM^{vac.} &= CBM^{bulk} + \Delta E^{CBM} + \Delta V. \end{aligned} \quad (2)$$

Step (i) was carried out using bulk models generated by *ab initio* simulations and, for comparison, by classical MD simulations. The calculation of ΔV involves the generation of MD trajectories of water slabs in contact with a relatively thick vacuum region, which are computationally expensive to obtain from *ab initio* simulations. To reduce the computational cost, we generated water slabs using classical potentials (TIP3P, TIP4P, and SPC/E) and we explored the possibility of computing ΔV for configurations extracted from classical MD trajectories. Our models consisted of 108 water molecules in contact with a vacuum region of ≈60 Å in a supercell of dimensions of $L_x = L_y = 12.77$ Å and $L_z = 80.0$ Å; the simulations were performed at 300 K for a total simulation time of ≈10 ns. The value of ΔV was computed as the difference in the average electrostatic potential $\overline{V}(z)$ between the region where the liquid is present and the vacuum region:

$$\overline{V}(z) = \left\langle \iint dxdyV(x,y,z)/A \right\rangle, \quad (3)$$

where A is the surface area of the water slab and z is the direction perpendicular to the water-vacuum interface. For each simulation, we used 50 configurations to evaluate $\overline{V}(z)$, chosen to be equally spaced in time over a trajectory of 10 ns.

Figure 2 shows the $\overline{V}(z)$ of three different water slabs generated using TIP3P, TIP4P, and SPC/E potentials. We found that the value of ΔV is insensitive to the choice of the classical potentials, yielding a value of 3.7 ± 0.05 eV, in good agreement with that reported in Ref. [35] ($\Delta V = 3.63$ eV) for a SPC/E water slab. We also computed ΔV for an ice Ih slab generated in an *ab initio* simulation at 150 K [36], and we obtained a slightly lower value of $\Delta V = 3.6$ eV. The weak sensitivity of ΔV to the force field is an important result from the computational standpoint, as it avoids the need to carry out full equilibrations of water slabs using *ab initio* simulations. In the following, we used the average value $\Delta V = 3.7$ eV for the evaluation of the positions of the VBM and CBM reported in Table I and Fig. 3.

While the average electrostatic potential entering Eq. (2) is fairly insensitive to the empirical potentials employed, we found that the electronic band gap shows a more complex variability. Table I shows results for the band gap and band edge positions of liquid water, computed at the PBE and G_0W_0 levels of theory for snapshots generated by classical and *ab initio* simulations. While TIP3P and TIP4P configurations yield band gaps in good agreement with that obtained

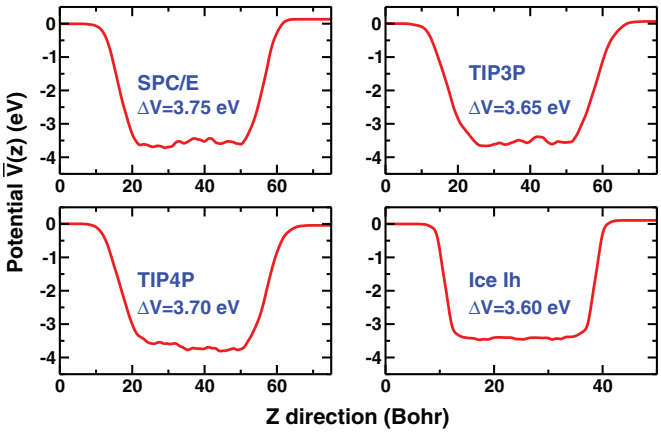

FIG. 2. (Color online) Planar average of the electrostatic potential [$\overline{V}(z)$] along the z direction of water slab models generated using different classical potentials (TIP3P, TIP4P, and SPC/E). The vacuum level is set at zero. The corresponding average values of the relative average electrostatic potential (ΔV) of the bulk and vacuum regions are presented, with an average fluctuation of ≈0.1 eV in all cases. The same quantity computed for an ice Ih slab is shown for comparison.

with *ab initio* configurations, SPC/E water models exhibit a smaller (0.3–0.5 eV) band gap at both the PBE and G_0W_0 levels of theory. In particular, the G_0W_0 band gap of the SPC/E model shows the largest deviation from experimental values.

To understand why SPC/E water configurations exhibit the smallest band gap of all models, we investigated further how the liquid structure affects the calculated electronic gap. When the OH bond length of the SPC/E model was decreased from the original value of 1.0 Å to 0.957 Å (i.e., the OH bond length in the TIP3P and TIP4P water models), the PBE band gap of SPC/E water snapshots increased to 4.0 ± 0.2 eV, in agreement with values obtained for TIP3P and TIP4P configurations. We found similar results for the isolated water molecule, for which the computed HOMO-LUMO gap decreased by ≈0.23 eV when the OH bond length increased from 0.957 Å to 1.0 Å. These results indicate that the effect of the intra-molecular

TABLE I. Positions of the valence band maximum (VBM) and conduction band minimum (CBM) of liquid water with respect to the vacuum level, computed at the PBE and G_0W_0 levels of theory for configurations obtained from first-principles (PBE) and classical (SPC/E, TIP3P, and TIP4P) MD simulations. Experimental results for the VBM are −10.06 eV [5,6], −9.9 eV [9], and −9.3 eV as inferred from the experimental results reported in Ref. [9]. The experimental results for the CBM are −1.2 eV [10,11] and −0.74 eV [4].

	SPC/E	TIP3P	TIP4P	PBE
PBE				
VBM	-5.9 ± 0.1	-6.1 ± 0.1	-6.1 ± 0.2	-6.1 ± 0.1
CBM	−2.2	−2.0	−2.0	−1.9
Band gap	3.7 ± 0.1	4.1 ± 0.1	4.1 ± 0.2	4.2 ± 0.1
G_0W_0				
VBM	-8.7 ± 0.2	-9.0 ± 0.2	-9.0 ± 0.2	-8.8 ± 0.2
CBM	−0.9	−0.7	−0.7	−0.7
Band gap	7.8 ± 0.2	8.3 ± 0.2	8.3 ± 0.2	8.1 ± 0.2

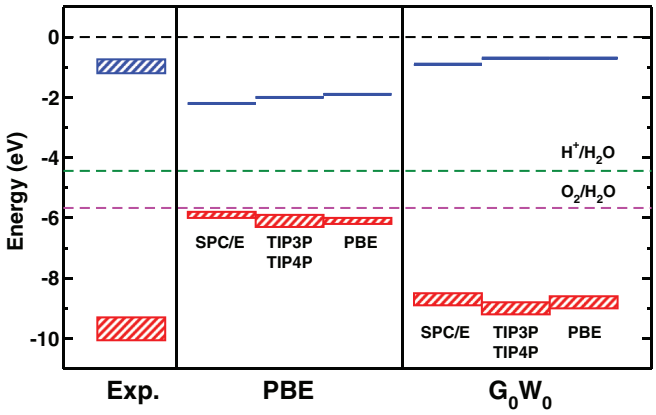

FIG. 3. (Color online) Positions of the valence band maximum (thick red lines) and conduction band minimum (thick blue lines) of liquid water with respect to the vacuum level computed at the PBE (middle panel) and G_0W_0 (right panel) levels of electronic structure theory (see Table I), compared to experiments [4–6,9–11] (left panel). The vacuum level, reduction and oxidation potentials of water [37] are indicated by the dashed black, green, and magenta lines, respectively. We show values obtained using water configurations extracted from first-principles (PBE) and classical (SPC/E, TIP3P, and TIP4P) MD simulations.

structure on the liquid band gap is not negligible (of the order of 0.3−0.5 eV).

The temperature and water density used to generate configurations in MD simulations also affects the calculated gap. For example, the PBE band gap of configurations generated by *ab initio* MD simulations slightly increases with decreasing temperature (4.2 ± 0.1 eV at 390 K and 4.5 ± 0.1 eV at 317 K for configurations at the experimental density of 1.1 g/cm^3) and with increasing density (3.9 ± 0.1 eV at 0.85 g/cm^3 and 4.2 ± 0.1 eV at 1.1 g/cm^3 for configurations generated at $T = 390$ K). Our calculations thus indicate that the overall variation in the band gap of the liquid may be as large as 0.7 eV, depending on the level of theory, and on the specific thermodynamic conditions used to generate liquid water configurations.

We now turn to the comparison of the computed band edge positions with experimental results. Similar to the band gap, the band edge positions obtained with TIP3P, TIP4P, and *ab initio* configurations are in agreement within 0.2 eV. In the following we focus on the results computed for configurations obtained from *ab initio* simulations.

As shown in Table I, the positions of the VBM and CBM predicted by the PBE functional severely deviate from experiment [38], in particular the VBM position is qualitatively incorrect, as it lies only ≈0.5 eV below the experimental water oxidation potential. Instead, a satisfactory agreement is obtained when the G_0W_0 approach is employed. When compared to the value reported by Winter *et al.* [9], the position of the VBM computed by MBPT for *ab initio* configurations is still ≈1.1 eV too high. As discussed in the introduction, if a power law of the type $Y \sim (E - E_t)^2$ were used to describe the photocurrent in the region near the threshold energy, a value of $E_t = 9.3$ eV would be obtained. Using this value for the threshold energy, the agreement between our theoretical results and experiment is within 0.5 eV for the position of the VBM (see Table I). Since G_0W_0 calculations probe the photocurrent onset, i.e., the very top of the valence band, the value $E_t = 9.3$ eV appears to be appropriate for a comparison with our results. The remaining discrepancy with experiments may stem from experimental conditions, e.g., possible electrokinetic charging effects in the experiments [39,40] that are not present in the calculations. Discrepancies could also be due to the neglect of off-diagonal matrix elements in the self-energy and the use of approximate PBE wave functions as input in G_0W_0 calculations. In particular, it was shown that by taking into account off-diagonal matrix elements of the self-energy [41] or by using PBE0 wave functions as input [42], the value of the HOMO of an isolated water molecule decreases by ≈0.3–0.4 eV compared to the one obtained with PBE wave functions, resulting in a better agreement with experiment.

While the use of PBE0 wave functions may affect the valence band position obtained with G_0W_0, we expect that the CBM position would be weakly modified by the use of PBE0, as the LUMO of water is a delocalized state [43]. Therefore we consider our result for the position of the CBM, −0.7 eV, to be in reasonable agreement with the −0.74 eV estimate proposed in Ref. [4]. We suggest that experimental results putting the CBM at −1.2 eV may possibly be probing presolvated electron states and not the CBM of the neutral liquid.

In summary, we reported the first theoretical determination of the positions of the VBM and CBM of liquid water using many-body perturbation theory coupled with *ab initio* MD simulations, and we presented a comprehensive analysis of the effect of structural models on the electronic properties of the liquid. We showed that the positions of the VBM and CBM predicted by DFT with a semilocal density functional are qualitatively incorrect, and the use of MBPT is crucial to obtain (semi)quantitative agreement with experiments. We found that intramolecular structural effects and variation of temperature and pressure close to ambient conditions may lead to variations of the water band gap of 0.3−0.7 eV. We also showed that the structure of water slabs, used to compute the position of the vacuum level, may be conveniently generated using classical force fields, in particular the TIP3P and TIP4P empirical potentials, thus leading to substantial computational savings. Our interpretation of experiments, especially the position of the CBM, and our assessment of the level of theory necessary to describe the electronic properties of water, represent an important step towards building a robust computational scheme to investigate the electronic structure of aqueous interfaces, and the position of the water redox potential relative to the band edges of semiconductors and insulators.

We thank Deyu Lu for useful discussions. Part of this work was performed under the auspices of the US Department of Energy by Lawrence Livermore National Laboratory under Contract No. DE-AC52-07NA27344; part of this work was supported by DOE/BES (Grant No. DE-SC0008938) T.A.P. acknowledges support from the Lawrence Scholar program.

[1] M. G. Walter, E. L. Warren, J. R. McKone, S. W. Boettcher, Q. Mi, E. A. Santori, and N. S. Lewis, Chem. Rev. **110**, 6446 (2010).
[2] L. Turi and P. J. Rossky, Chem. Rev. **112**, 5641 (2012).
[3] C. E. Krohn, P. Antoniewicz, and J. Thompson, Surf. Sci. **101**, 241 (1980).
[4] A. Bernas, C. Ferradini, and J.-P. Jay-Gerin, Chem. Phys. **222**, 151 (1997).
[5] P. Delahay and K. Von Burg, Chem. Phys. Lett. **83**, 250 (1981).
[6] P. Delahay, Acc. Chem. Res. **15**, 40 (1982).
[7] A. Brodsky and A. Tsarevsky, J. Chem. Soc., Faraday Trans. 2 **72**, 1781 (1976).
[8] B. Winter and M. Faubel, Chem. Rev. **106**, 1176 (2006).
[9] B. Winter, R. Weber, W. Widdra, M. Dittmar, M. Faubel, and I. Hertel, J. Phys. Chem. A **108**, 2625 (2004).
[10] D. Grand, A. Bernas, and E. Amouyal, Chem. Phys. **44**, 73 (1979).
[11] A. Bernas, D. Grand, and E. Amouyal, J. Phys. Chem. **84**, 1259 (1980).
[12] J. Schnitker, P. J. Rossky, and G. A. Kenney-Wallace, J. Chem. Phys. **85**, 2986 (1986).
[13] L. Hedin, Phys. Rev. **139**, A796 (1965).
[14] M. S. Hybertsen and S. G. Louie, Phys. Rev. Lett. **55**, 1418 (1985).
[15] V. Garbuio, M. Cascella, L. Reining, R. DelSole, and O. Pulci, Phys. Rev. Lett. **97**, 137402 (2006).
[16] D. Lu, F. Gygi, and G. Galli, Phys. Rev. Lett. **100**, 147601 (2008).
[17] C. Zhang, T. A. Pham, F. Gygi, and G. Galli, J. Chem. Phys. **138**, 181102 (2013).
[18] F. Gygi, Qbox, a Scalable Implementation of First-Principles Molecular Dynamics, http://eslab.ucdavis.edu
[19] J. P. Perdew, K. Burke, and M. Ernzerhof, Phys. Rev. Lett. **77**, 3865 (1996).
[20] D. Vanderbilt, Phys. Rev. B **32**, 8412 (1985).
[21] All hydrogen atoms were replaced with deuterium in order to maximize the allowable time step; we adopted a time step of 10 a.u. in all simulations.
[22] J. A. Morrone and R. Car, Phys. Rev. Lett. **101**, 017801 (2008).
[23] J. C. Grossman, E. Schwegler, E. W. Draeger, F. Gygi, and G. Galli, J. Chem. Phys. **120**, 300 (2004).
[24] E. Schwegler, J. C. Grossman, F. Gygi, and G. Galli, J. Chem. Phys. **121**, 5400 (2004).
[25] W. L. Jorgensen, J. Chandrasekhar, J. D. Madura, R. W. Impey, and M. L. Klein, J. Chem. Phys. **79**, 926 (1983).
[26] H. J. C. Berendsen, J. R. Grigera, and T. P. Straatsma, J. Phys. Chem. **91**, 6269 (1987).
[27] H.-V. Nguyen, T. A. Pham, D. Rocca, and G. Galli, Phys. Rev. B **85**, 081101 (2012).
[28] T. A. Pham, H.-V. Nguyen, D. Rocca, and G. Galli, Phys. Rev. B **87**, 155148 (2013).
[29] H. F. Wilson, F. Gygi, and G. Galli, Phys. Rev. B **78**, 113303 (2008).
[30] H. F. Wilson, D. Lu, F. Gygi, and G. Galli, Phys. Rev. B **79**, 245106 (2009).
[31] J. P. Perdew, M. Ernzerhof, and K. Burke, J. Chem. Phys. **105**, 9982 (1996).
[32] C. Adamo and V. Barone, J. Chem. Phys. **110**, 6158 (1999).
[33] J. Heyd, G. E. Scuseria, and M. Ernzerhof, J. Chem. Phys. **118**, 8207 (2003).
[34] M. A. L. Marques, J. Vidal, M. J. T. Oliveira, L. Reining, and S. Botti, Phys. Rev. B **83**, 035119 (2011).
[35] K. Leung, J. Phys. Chem. Lett. **1**, 496 (2010).
[36] T. A. Pham, P. Huang, E. Schwegler, and G. Galli, J. Phys. Chem. A **116**, 9255 (2012).
[37] S. Trasatti, Pure Appl. Chem. **58**, 955 (1986).
[38] J. Cheng and M. Sprik, Phys. Chem. Chem. Phys. **14**, 11245 (2012).
[39] A. M. Duffin and R. J. Saykally, J. Phys. Chem. C **111**, 12031 (2007).
[40] N. Preissler, F. Buchner, T. Schultz, and A. Lübcke, J. Phys. Chem. B **117**, 2422 (2013).
[41] C. Rostgaard, K. W. Jacobsen, and K. S. Thygesen, Phys. Rev. B **81**, 085103 (2010).
[42] F. Bruneval and M. A. L. Marques, J. Chem. Theory Comput. **9**, 324 (2013).
[43] The IPR (inverse participation ratio) ratio between HOMO and LUMO wave functions of *ab initio* water configurations is ≈210. The IPR of a wave function ψ is defined as $\mathrm{IPR} = \frac{\frac{1}{N}\sum_{i=1}^{N}|\psi(r_i)|^4}{[\frac{1}{N}\sum_{i=1}^{N}|\psi(r_i)|^2]^2}$ where N is the number of points in the real-space grid used to represent the wave function. An IPR value of 1 indicates that the wave function is completely delocalized and the value increases from 1 with the localization of the wave function.